Shell structures

Daan Dekker
Shael Hakimi

Course CT3280 Shell Roofs
Delft University
Department of Civil Engineering and Geosciences

January 2024

Contents

1 Introduction

In this report, we present the design and testing of a shell structure model. The document is authored in the context of the Bend and Break shell structure course.

The primary objective of this report is to accurately predict the bearing capacity of the shell structure model. This entails the creation of a shell structure design and utilizing both software and manual calculations to assess the strength of the structure. The model is conceived based on fundamental principles of shell structures.

The structure of the report is organized as follows: Chapter 2 provides background information on shell structures, serving as the foundation for the subsequent model design detailed in Chapter 3. In Chapter 4, a stress analysis is conducted for the model, presenting calculations pertaining to its strength in order to predict bearing capacity. Chapter 5 showcases the results of the load test applied to the model. Chapter 6 comprises the Discussion section, where differences and similarities between calculations and results are analyzed. Chapter 7 evaluates the feasibility of scaling up the model in real-life applications. The final chapter, Chapter 8, encompasses the Conclusion.

2 Background information shell structures

In this chapter some background information of shell structures is described. Not all information of shell structures is presented, but only some basic information which helps with designing the shell structure.

2.1 Type of shell structure

A shell structure is characterised by a curved, shell like form. The form of a shell structure allows the design to be very thin compared to its dimensions. Loads on the shell structure can be dissipated in different directions to the foundation. This makes a shell structure an efficient design. In this report a difference between two different shell structures is made. Solid shell structures and grid shell structures.

2.1.1 Solid shell structures

The name solid shell structure already describes the definition of the type of structure. A solid shell structure consists of a self supportive shell which transfers the load through the shell to the foundation. An example of an solid shell structure can be seen in figure 1. A lot of solid shell structures are made out of concrete, because it can be poured in many shapes and has an high compressive strength. The use of a solid shell structure gives a lot of room to design with. A design can have curves in not more than one direction, which lead to interesting designs as can be seen in the figure.

Figure 1: solid shell structure made out of concrete

2.1.2 Grid shell structure

A grid shell structure is a structure that consists of single members in an lattice configuration that forms a curving surface. An image of a grid shell structure can be seen in figure 2. Using geometry many shapes of shells can be made. The grid consists of members that cross each other. A grid shell structure weighs less than an solid shell and uses less material in most cases. Therefore it is a efficient method to design with.

Figure 2: grid shell structure made out of wood

2.1.3 Materials

There are different types of materials that can be used to make a shell structure. The type of material which is best to use depends on the type of shell. For an solid shell structure, concrete is a good option. Concrete can be poured in liquid state, which allows for a lot of choiche in shape. Concrete has great compressive strength. The tension in the reinforcement concrete shell structure is absorbed by the reinforcement steel.

For a grid shell structure wood and steel are a good option to use. By laying wooden slats in a grid, you can make a light grid shell structure. Wood can absorb tension and compression stresses, just like steel. Wood is less expensive and weighs less than steel. It is however more difficult to bend wood than steel. Steel bars will also be stronger than wooden slats. For a shell structure with long dimensions, steel is also a better option, because of the bearing capacity but also the availability of the length of the bars. Long lengths of wood can not be rough sawn, but have to be laminated out of smaller wooden slats. This is more expensive.

3 Model design

In this chapter the design of the model that will be tested is shown. The design of the model is based on the basic knowledge described in chapter 2. For the model a grid shell structure is chosen to design with. This is done because the many interesting shapes you can build with it and the fact that it is easier to adjust than a concrete shell structure.

In this chapter, the exposition of the model's design intended for testing purposes is presented. The conceptualization of the model is rooted in the foundational knowledge elucidated in Chapter 2. A deliberate choice has been made to employ a grid shell structure for the model's design, owing to its versatility in constructing intriguing forms and its comparative ease of adaptability when juxtaposed with a concrete shell structure.

The primary objective guiding the design process is to achieve an optimal distribution of forces while ensuring simplicity in fabrication. The selection of a dome structure aligns with this objective, as dome shell structures inherently distribute loads uniformly across their surfaces, thus facilitating efficient load transfer mechanisms. To preserve the grid element within this form, careful considerations are made regarding the inter-lattice distance, cross-sectional area, and dome diameter. Specifically, a diameter of 60 cm and a heart-to-heart distance of 5 cm have been chosen for the shape. The lattice dimensions are specified as 10x5 mm.

The chosen 60 cm diameter is deemed sufficiently expansive to accurately represent the essential features and structural elements of the dome grid shell structure, all the while remaining manageable for testing purposes. The curvature of the slats is set at a radius of 370 mm, an unusually high curvature for wood, yet instrumental in imparting an elegant and distinctive character to the structure. The inter-lattice distance provides space to apply the distributed load by tying ropes to the intersections of the slats.. For a visual representation of the final design, please refer to Figure 3.

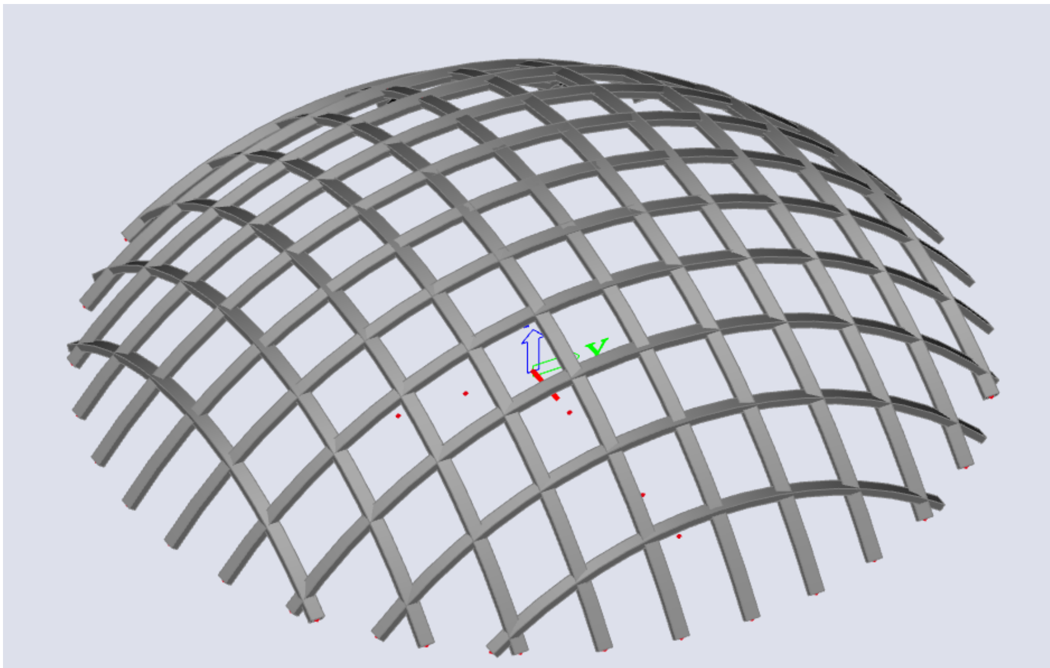

Figure 3: Final design of the shell structure, using a distance between lats of 5 cm and a diameter of the dome of 60 cm.

4 Stress analysis

The stress analysis of the grid shell structure are described in this chapter. The calculations are based on the model presented in chapter 3. The goal of the stress analysis is to predict the stresses in the shell structure at a given load and to predict the bearing capacity of the structure. The stress analysis contains of an SCIA model similar to the model and hand calculations. With both these techniques some assumptions have to be made, which will be explained at each sub chapter.

4.1 SCIA Engineer analysis

A stress analysis of the model is made using SCIA Engineer. For this model, some assumptions are made regarding the boundary conditions and loads. In the model, hinged rigid supports are used at the end of each member, such that the rotation around any axis is free and the translation in any direction is restricted. The reasoning behind this assumption is that in the practical model, the ends of the slats are screwed down to the platform on which the shell structure is standing, in this way, rotation is possible but translation not. In the figure below, the hinged supports are visualized.

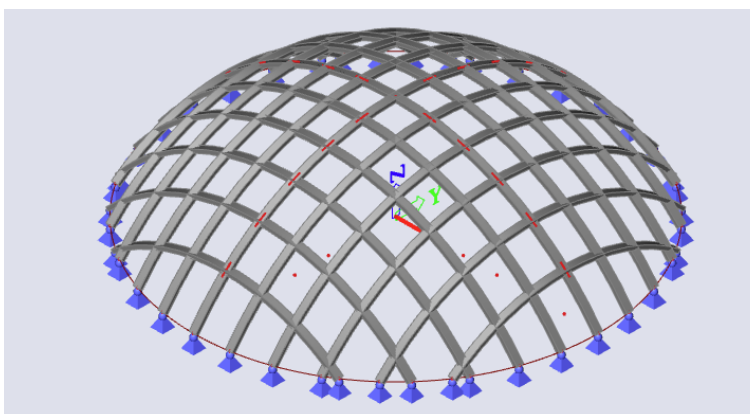

Figure 4: The visualization of the hinged supports of the model in SCIA Engineer

The other assumption that is made is that a line load is applied on every member. The final assumption, which was also checked by the the manual calculations in subchapter 4.2, is that the structure will fail on buckling.

With a mesh of 2 cm, and a small scale for the structure (so how it is built in the test), the following results are obtained regarding stress values with a line load (q) on each member of 0.41 kN/m. This is the maximal load at which the structure will not buckle.

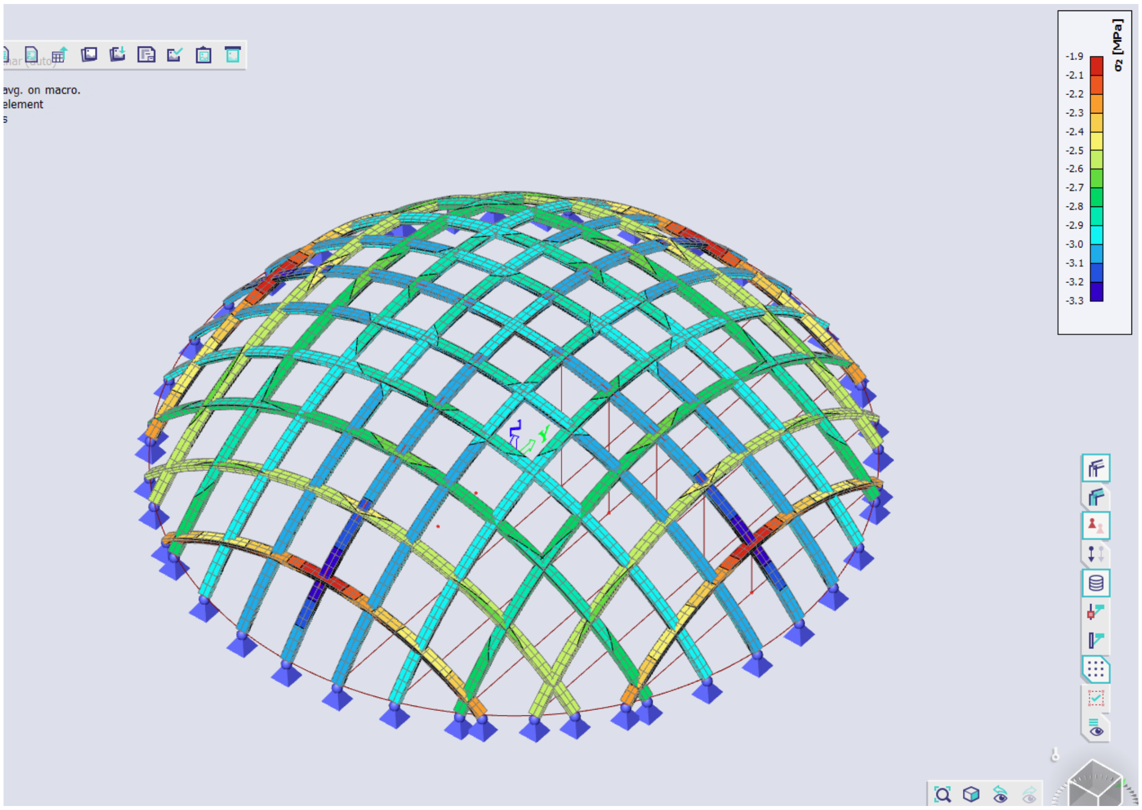

Figure 5: Stress analysis of the structure (principal magnitudes, σ_2)

For the rest of the report, the results obtained from the SCIA engineer analysis will not be used, the discussion chapter will have further information regarding this topic.

4.2 Manual calculation

In this subsection, the maximum permissible load will be determined through manual calculations. The assumption is made that the load on the longest member will be determinative for the rest of the construction. Initially, the maximum load, considering the maximum compression of wood, will be computed. Subsequently, this value will be compared with the maximum load at which structural buckling occurs, thereby establishing the determinative load. Lastly, the maximum load will be ascertained based on this determinative load. All of these manual calculations can be found in appendix A.

4.2.1 Maximum load based on maximum compression of wood

Figure 6 shows the specification parameters of the member, which will be needed for the calculation of the maximum load.

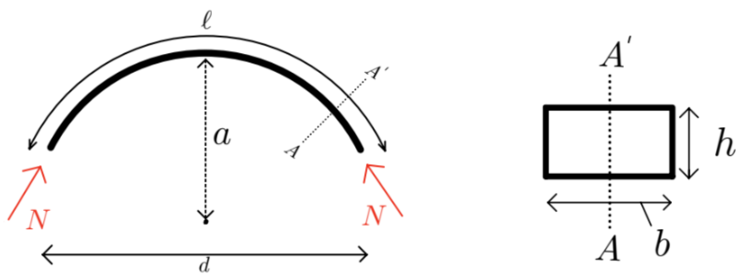

Figure 6: Specification parameters of a member, in which a refers to the curve radius, d to the horizontal length, l to the length of the member, b the width and h the height of the cross-section, and N the reaction forces on the supports.

The reactions at the supports (N) can be calculated with the following formula.

$$N = \sigma_{compression} \cdot (b \cdot h) \tag{1}$$

In which:

- $\sigma_{compression}$ is the maximal compressive strength of the member. (kN/m^2)
- $(b \cdot h)$ is the cross-section area of the member. (m^2)

Now the maximal line load on the member (q) can be calculated using the following formula.

$$q = \frac{N}{a} \tag{2}$$

In which:

- N is the reaction force, calculated in formula 1. (kN)
- a is the radius of curvature of the member. (m)

Now, the values of the reaction forces at the supports (N) and the maximal line load (q) can be calculated. The type of timber used is C24, which has an $\sigma_{compression}$ of 51 N/mm^2. The specification parameters are shown in table 1, and the results are shown in table 2.

parameter	value (mm)
d	600
l	700
b	10
h	5
a	369.63

Table 1: Specification parameters of the longest member in the structure.

N	2.55 kN
q	6.70 kN/m

Table 2: Results of the reaction force at the supports and the line load.

The line load by which the structure will fail due to crushing of the wood is 6.70 kN/m. By multiplying this number by the total lengths of all the slats, you get the total force the structure can carry. This is 86.86 kN for a distributed load. This is equivalent to 8836.38 kg, which is really a lot for a wooden grid shell structure. Therefore is is assumable the structure will not fail on crushing of the wood, but on buckling. Therefore a calculation for the buckling load is made below.

4.2.2 Maximum load based on buckling

The reaction forces at the supports (N) based on buckling can be calculated using the following formula.

$$N = \frac{\pi^2 EI}{L^2} \tag{3}$$

In which:

- E is the Young's Modulus. (N/mm^2)
- I moment of inertia of the member, in this case $\frac{bh^3}{12}$. (mm^4)
- L is the buckling length. (mm)

The buckling length is a parameter which you can choose in different ways; based on a FEM analysis, based on the distance of one member (member is the distance of a slat between two crossings) or choosing half of the whole arch because a member often buckles in the middle (like a three hinge truss). In this case the assumption is made that the buckling length will be half of the length of the longest arch, which is 350 mm.

Now, the line load (q) can be calculated using formula 3 and 2, which is explained in subchapter 4.2.1.

Finally, the reaction forces at the supports and the line load are put in table 3. For a buckling length of 6 members/350 mm. This results in a line load of 0.227 kN/m working on all the slats. This is equivalent to a resultant force of 2852.96 N, or 290.82 kg.

N	0.083 kN
q	0.227 kN/m

Table 3: Results of the reaction force at the supports at

4.2.3 The determinative maximum load

The reaction forces at the supports based on the maximum compression of wood and the buckling can now be compared, the lowest one yields the determinative maximum load. Table 2 and 3 show the maximum permissible loads, and in this case the maximum permissible buckling load is the lowest, so this one is determinative.

Now, the final load (m in kg) can be calculated using the following formula.

$$m = \frac{q \cdot l_{total}}{g} \tag{4}$$

In which:

- q is the determinative line load.
- l_{total} is the length of the line load.
- g is the gravity constant 9.81 m/s^2.

Because of the line load on each member of the structure, the length of the line load will be the sum of the length of each member.

The final result of the maximum load is thus $m = 290\ kg$, concluding that the structure will buckle at this load.

4.2.4 Point load

In the case that the structure does not buckle at the given value of the load in sub chapter 4.2.3, a point load will be applied until failure. The point load is applied at the top of the structure. The point load is not exactly a point, but a line load over a small distance (70 mm). With this difference of load application, the resultant force calculated in sub chapter 4.2.3 will be different. The calculation for buckling and compression stay the same, only the line load is not multiplied by the total length of all the slats as by a distributed load. Instead the line load is multiplied by four times 70 mm. This is the contact area between the point load and the wooden slats.

For the resultant force whereby the wood will fail on crushing the value will change from 86684.85 N (for distributed load) to 1931.67 N (for point load). This is equivalent to a weight of 191.91 kg.

For the resultant force whereby the wood will fail on buckling the value will change from 2852.96 N (for distributed load) to 2288 N (for point load). This is equivalent to a weight of 233.30 kg, for a buckling length of one member (58.33 mm).

With these new values, the structure will fail on crushing of the wood. At a resultant force of 2288.96 N.

5 Results

In this chapter the results of the distributed and point load test are shown. For both the tests the deflection of the structure was measured at the top of the structure. The load at which the structure collapsed is also shown for both structures.

5.1 Results distributed load

In this subsection, the results regarding he distributed loads will be shown, this includes the deflection and collapsing load.

5.1.1 deflection distributed load

The first test on the structure was with a distributed load. The distributed load was simulated by putting weights on every of the laths. A picture of the structure including the ropes to hold the weights can be seen in figure 7. The deflection of the structure was measured at the top of the structure with an analog dial indicator. The displacement at the top was measured at every 16 kg of weight which was added. The deflection diagram can be seen in figure 8. The deflection of the structure is displayed in 0.01 mm. The total deflection is 0.7 mm. The deflection curve appears to have an linear relationship. Therefore a trend line is plotted, so deflection out of the range of the measurements can be predicted.

Figure 7: picture of the grid shell structure including the ropes that transfer the weights at the bottom into a distributed load

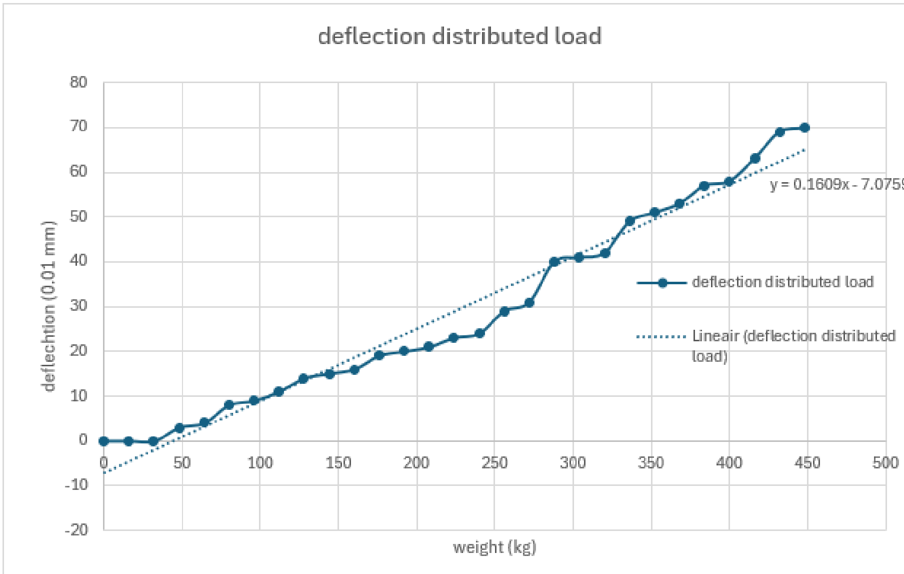

Figure 8: deflection of structure loaded with distributed load

5.1.2 collapsing load distributed load

The structure did not collapse under a distributed load. This was somewhat remarkable, because there was no other wooden grid shell structure which did not collapse under a distributed load. The test stopped at 509 kg. The deflection at this point was very minimum, and the structure gave no sign of collapsing.

5.2 Results point load

The grid shell structure did not collapsed under a distributed load. Therefore the structure was tested with a point load at the top of the structure. This point load was applied at the top of the structure. The results of this test are shown below.

5.2.1 deflection point load

The deflection due to the point load is done the same as with the distributed load. The deflection was again measured at the top of the structure. The deflection diagram can be seen in figure 9. Compared to the deflection under a distributed load, the deflection under a point load is much greater. The maximum deflection measured was 337 mm at a weight of 112 kg. At 112 kg the deflection increased continuously until the structure collapsed. The deflection curve appears to have a linear relationship, just as in figure 8 with the distributed load.

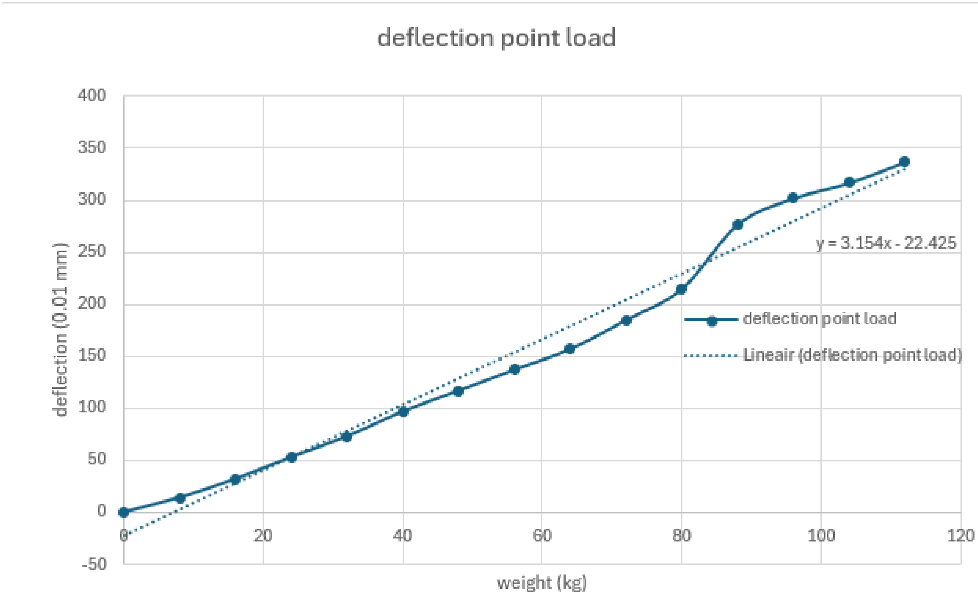

Figure 9: deflection of structure loaded with point load

5.2.2 collapsing load distributed load

The structure did collapse at a point load of 117 kg. This weight was distributed over a length of 50 mm. The structure did collapse due to buckling which was followed by breaking of the laths. A picture of the structure after collapsing can be seen in figure 10. The laths buckled over a length of 3 members, which is the same as 17.5 cm. The laths did not break at an instant. The laths slowly yield until the deflection became to much and the structure collapsed. Only the top of the structure collapsed. The rest of the laths where completely intact.

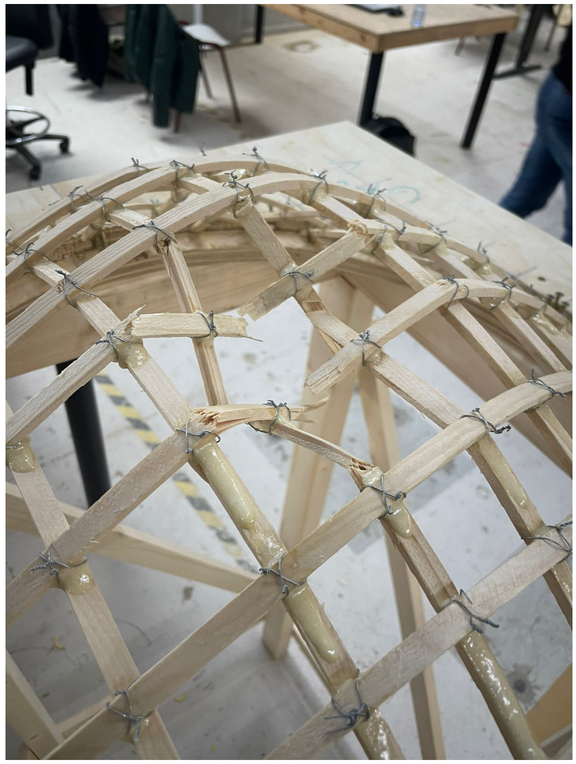

Figure 10: a picture of the structure after collapsing due to point load

6 Feasibility

In this chapter the feasibility of the structure is discussed. Hereby the feasibility of building the structure will be discussed, but also the scale it could be build with.

6.1 Feasibility of building

The structure that was build as a model consists of wooden laths that are bend with a radius of 15.37 cm. This is a really big radius for wood to be bend in. In practice it would be very difficult to bend the lumber in this radius. A better option would be to laminate wood. This means small strips of wood are glued to each other in the desired form. This makes a strong beam and also gives the option to make longer beams. If the model would be build on a 1:10 or even 1:100 scale, the dimensions of the lumber would be far greater. The option of solid rough sawn wood would not be feasible, because there are no lengths of beams that long. The best option is then to use Glue Laminated (GluLam) beams. These beams would be plenty strong enough, because modern day glue is stronger than the connection between the wood grains.
Another part that could be difficult to execute in real life is the connections between the slats. In the model the connections are made by tying iron wire around the crossings, and adding wood glue. The wood glue gives a really strong connection between the slats. The iron wire gives clamping pressure, so the wood glue can cure. In reality the wood glue can be realised, but the iron wire is difficult to execute. The cross-section of the lumber will increase, and therefore the iron wire needs to be longer and thicker. This makes it more difficult to pull the wire tied so it clamps the wood together. A better option would be to big wood screws or bolts to connect the wooden laths to each other. A schematic drawing o connection with steel plates and bolts that could be used in real life is shown in figure 11.

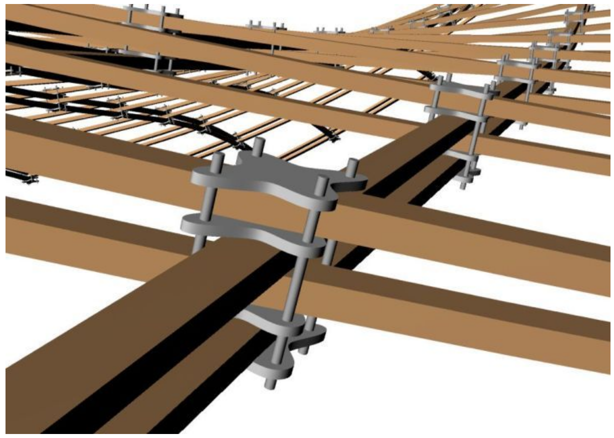

Figure 11: connection between wooden slats in grid shell structure using metal plates and bolts

6.2 Scaling

In this subsection, we delve into the topic of model scaling, examining the permissible scale at which the model can be constructed. Additionally, an analysis of real-life structural performance, considering factors such as displacement and stresses, is conducted.

To determine the feasible scale for constructing the model in reality, we rely on the outcomes of the model's simulations. The grid shell structure, in these simulations, demonstrated a capacity to withstand an evenly distributed load of 509 kg. The surface area of the structure is determined using a specific equation, resulting in a surface area of 0.58 m^2. The self-weight of the shell structure, at 0.314 kg, translates to a self-weight per roof area of 0.00314 kN/ 0.58 kg = 0.0054 kN/m^2. Notably, the model exhibited resilience to a load of 509 kg evenly distributed, equivalent to 8.78 kN/m^2, aligning with scaling principles.

Further considerations involve the actual shell's capacity to support its own weight and an additional snow load of 1 kN/m^2. The scale factor, as calculated in Equation 6, provides insight into the multiplicand for the model's dimensions. For the specific model in question, the scale factor is determined to be 626, indicating that the real structure can be constructed at a size 626 times larger than the model.

Consequently, the envisaged real-world model can accommodate dimensions such as a radius of 375.6 meters and a height of 96.22 meters. Despite the seeming enormity for a wooden slat structure, the combination of extreme curvature and robust adhesive connections optimizes load distribution, rendering such dimensions feasible. The deflection of the real size structure can be predicted by multiplying the deflection of the model by 509 kg by a factor of 626. This results in an deflection of 438.2 mm. This deflection is way to much in case for a floor, but because the shell would probably be used as roof it can be acceptable, with regard to the span of the roof. The deflection can be reduced by adding columns.

$$A = 2 * \pi * R * h \tag{5}$$

- A = surface area (m^2)
- R = radius (m)
- h = height of the dome (m)

$$distributedloadonmodel/s = n * selfweightstructure + snowload \tag{6}$$

- distributed load on model = 8.78 kN/m^2, known from testing model
- s = safety factor (in this case 2)
- n = scale factor
- self weight structure = 0.0054 kN/m^2
- snowload = 1 kN/m^2

7 Discussion

In this chapter the results and the effects on the results are discussed. In this project a lot of factors had influence on the predictions and performance of the structure. This chapter is divided in several subjects of what had influence on the model.

7.1 Stress analysis

In this subsection all assumptions and methods of calculation/modelling is discussed. The modelling part consisted of a SCIA Engineer model and a manual calculation.

7.1.1 SCIA Engineer analysis

For the modelled structure in SCIA Engineer, assumptions are made regarding the boundary conditions, mesh and following results.

An assumption was made that at every member has two hinged supports at it's ends (see figure 4) which are rigidly fixed to the ground, allowing only rotation but restricting translation. This assumption was made with the reasoning that the slats are screwed down on each side. In reality, these "hinged supports" were constructed as shown in the following figure (12).

Figure 12: The practical solution for connecting slats to the frame, using screws and glue on each end of the slat.

The chosen rigid hinged support is not completely according to reality, because the screws can only restrict translation to a certain extend. That is the reason why glue was also used, to further stimulate the restriction of the slat. In reality, this also affects the freedom of rotation of the slats, which is not taken in account in the SCIA Engineer analysis.

For the model load, an assumption was made regarding the type of load that was applied. In the SCIA Engineer, a line load was applied on each member. In reality, knots were placed on each crossing of two members (see figure 13), resulting in so-called "point loads" on each of these crossings. A line load is more distributed on the slat, while a point load at the location of each knot is not. So the latter mentioned load will be more susceptible to buckling than a more distributed load.

Figure 13: A picture of the built model from the top view, in which the (yellow) tie knots are shown on each crossing of two members.

The SCIA Engineer model was built on the small scale (so how the structure was built for the test). This has effects on the results obtained from the SCIA analysis, as the SCIA program is designed for real sized structures. Small structures may exhibit different material behavior at a smaller scale. Also, the impact of boundary conditions becomes more pronounced when dealing with smaller structures. This is because small structures have concentrated loads or supports in a relatively small area, leading to more localized effects.

7.1.2 Manual calculation

In the manual calculation, the longest slat (in the middle of the structure) is assumed to be determenative for the rest of the structure. This assumption was made based on the knowledge that in general longer slats are more susceptible to buckling and deflection. The buckling length was assumed to be half the length of the longest slat in the structure. However, the slat can have different buckling lengths also. Another one of these likely buckling lengths is the distance between two members, which is in our case 5 cm. This is because the force on a crossing between two members, can exceed the limit and break at that point, so the buckling length will be the distance between members.

A manual point load calculation was also made. This point load was modelled as a line load with the length of 70 mm on 4 members, this was done because the point load was applied through a wooden round plate (see figure 14).

Figure 14: The wooden plate (d=70 mm) used for the point load test.

7.2 Discussion building

Small imperfections at the building stage can have big influence on the performance of the model. In this subsections these imperfections and the influence of them are discussed.

The longest lat in the model is assumed to be the only one, but in reality there are multiple lats running beneath this lat. This changes the expected buckling failure, as the lats beneath support the loaded lat, reducing the chance of buckling failure.

The model is made of wooden slats that are bend with a radius of 153.7 mm. This is really a big curve for wood to make. This bend is made by hot steaming the wooden slats and bend it into place. This could have weakened the strength of the wood, which could lead to an early failure. The imperfections in the wood itself could also be a reason for an early collapse. A knot in a slat for example weakens the strength of the slat. These imperfections had not a great influence on the model in this project. The wooden slats where carefully selected and bad slats where discarded.

The connections between the slats are made by gluing the pieces together and applying clamping force with iron wire. This makes all of the wooden slats work together as a grid shell. The problem is that if the glue plus tie connections fails prematurely, the wooden slats do not work together as a solid structure. This will cause for an earlier collapse. In this model this problem was not an issue. Due to the strength of modern day glue the connections where strong enough to carry the load.

Another issue that can influence the performance is the alignment of the wooden slats. The wooden slats are modelled to be places 5 cm next to each other. In practice this distance can vary slightly between the slats. This problem can not be directly solved. It is important to build the model carefully and as accurate as possible. For precision jigs, to keep the slats in place, can be help full to ensure the accuracy of the model.

The last factor that could influence of the performance is the way the load is applied. As discussed in subsection 7.1 the load is applied using a string at each crossing of slats. All these strings eventually are all connected to one iron rod that carries a platform. It is important that the model fails, before the strings and connecting beams fail. In this project this was a great success. The platform plus strings and connecting beams where very well build and could hold way more than the load applied on the model. The position of the iron rod was also precisely below the middle of the structure, which means the resultant of all the forces on the model was at the right place (precisely in the middle of the structure). The wires and connecting beams did not interfere with each other, which also could influence the results. A picture of the model with the wires and connecting beams that transfer the load from the platform to the model can be seen in figure 15.

Figure 15: picture of the model and the wires and connecting beams that transfer the load from the platform to the model.

7.3 Discussion testing

During testing some factors could also influence the results. The model was first loaded with a distributed load. The load was constantly increased by putting extra weight on the platform. This was done by hand, which caused vibrations in the structure. This leads to higher forces and could have caused a premature collapse.

After the distributed load was applied, the model was still in tact. Therefore the structure was loaded with a point load at the top to see the shell collapse. The problem is that the effect of the distributed load could already have weakened the structure. This could have let to an early collapse with the point load.

Another issue that appeared during testing is that the point load applied at the top of the structure was not completely perfect placed. Precisely in the middle of the structure two slats cross each other. Therefore the point load needed to move slightly to the left. The point load is also not really a point. The point load is simulated by a disk with a radius of 70 mm which rests on 4 members of the slats.

7.4 Discussion of the results

In this chapter the results that came out of the testing are discussed. Mainly the effect of the factors discussed above are related to the results.

In chapter 5.1 the results of the test with the distributed load are shown. In this chapter the displacement at the top of the structure is displayed in the form of a graph. The total displacement at the top of the structure is 0.7 mm after 450 kg. This is really low displacement for the weight. With the point load, the maximal displacement of the top of the structure was 3.37 mm with a weight of 112 kg. This is approximately 5 times as great as with the distributed load. The main in the difference of the two deflections is the weight the load is applied. The distributed load, applies the load more evenly over the whole structure, while the point load causes really high stresses at the top of the structure.
The displacement dial could also have influence in the difference between the two displacement curves. With the distributed load, the dial was fully retracted in the beginning. The problem is that the displacement dial can not accurately measure small displacements.

8 Conclusion

In summary, the primary objective of this report has been the meticulous exploration of the design, construction, analysis, and testing of a shell structure, with a specific emphasis on pre-emptive estimation of its load-bearing capacity before experimental trials. The overarching aim has been to achieve a precise prediction of the structure's failure force, closely aligned with the actual load it can withstand during testing.

The constructed model in this report comprised wooden slats, each curved with a remarkable radius of 155 mm, a notably high curvature for wood. This distinctive design featured curved slats intersecting to form a rounded dome.

Through meticulous hand calculations, the load-bearing capacity of the shell model was determined, resulting in a resultant force (derived from a distributed force) of 2908.2 N. The actual load the shell structure successfully carried was 5090 N, at which point the structure remained intact.

To induce structural collapse, a departure from the distributed load was made, and a point load was applied instead. The structure exhibited failure under a point load of 1170 N, applied at the apex of the structure.

The model examined in this project has demonstrated the potential for real-life construction on a scale 626 times larger. Consequently, the envisaged dimensions for the actual structure include a radius of 375.6 meters and a central height of 96.22 meters. Noteworthy is the remarkable elevation for a wooden slat shell structure, a testament to the structure's substantial curvature and robust adhesive connections. These attributes contribute to the feasibility of such dimensions, resulting in the realization of an architecturally impressive building.

In conclusion, this project yielded a particularly unique shell model, achieving an almost implausible curvature in a wooden grid shell by maximizing the bending capacity of the wooden slats. Despite initial expectations, the wooden grid shell performed exceptionally well, matching or even surpassing the performance of conventional concrete structures.

A Manual structural calculations

In this section of the appendix, all manual calculation can be found regarding the distributed and point load.

A.1 Distributed load

```
% parameters
s= 0.1537; %hoogte in m
l = 0.6; %lengte in m
a = 0.5*s + (1/8)*(l^2)/s; %straal in m

b = 0.010; % breedte lat in m
h = 0.005; %hoogte lat in m
A = b*h; %oppervlakte in m2
I = (1/12)*b*h^3; %area moment of inertia lat

L_b = 0.35; %kniklengte in m

E = 10e9; %youngs modulus hout in Pa

sigma_c = 51e6; %maximale compressie hout in Pa

g = 9.81; %zwaartekrachtsversnelling in m/s2

%latlengtes hier plaatsen
l1 = 0.35661;
l2 = 0.49931;
l3 = 0.59280;
l4 = 0.65387;
l5 = 0.68869;

l6 = 0.70002;

l7 = 0.68869;
l8 = 0.65387;
l9 = 0.59280;
l10 = 0.49931;
l11 = 0.35661;

l12 = 0.35661;
l13 = 0.49931;
l14 = 0.59280;
l15 = 0.65387;
l16 = 0.68869;

l17 = 0.70002;

l18 = 0.68869;
l19 = 0.65387;
```

```
l20 = 0.59280;
l21 = 0.49931;
l22 = 0.35661;

%maximale load door maximale compression van hout
N_cmax = sigma_c*A; %normaalkracht in N
display(N_cmax);
q_cmax = N_cmax/a;
display(q_cmax);

%maximale load door buckling
N_bmax = ((pi^2)*E*I)/(L_b^2); %normaalkracht in N
display(N_bmax);
q_bmax = N_bmax/a;
display(q_bmax);

%totale load op structure (q_bmax bepalend bij Lb=30cm scia)
l_totaal = l1+l2+l3+l4+l5+l6+l7+l8+l9+l10+l11+l12+l13+l14+l15+l16+l17+l18+l19+l20+l21+l22;
m = (q_bmax*l_totaal)/g;
display(l_totaal)
display(m)
```

A.2 Point load

```
%parameters
s = 0.1537; %hoogte in m
l = 0.6; %lengte in m
a = 0.5*s + (1/8)*(l^2)/s; %straal in m

b = 0.010; % breedte lat in m
h = 0.005; %hoogte lat in m
A = b*h; %oppervlakte in m2
I = (1/12)*b*h^3; %area moment of inertia lat

L_b = 0.0583; %kniklengte in m

E = 10e9; %youngs modulus hout in Pa

sigma_c = 51e6; %maximale compressie hout in Pa

g = 9.81; %zwaartekrachtsversnelling in m/s2

F = 1931.5; %opgelegde kracht in N
b_last = 0.070; %de lengte van de last in m

%latlengtes hier plaatsen
l1 = 0.35661;
l2 = 0.49931;
l3 = 0.59280;
l4 = 0.65387;
```

```
l5 = 0.68869;

l6 = 0.70002;

l7 = 0.68869;
l8 = 0.65387;
l9 = 0.59280;
l10 = 0.49931;
l11 = 0.35661;

l12 = 0.35661;
l13 = 0.49931;
l14 = 0.59280;
l15 = 0.65387;
l16 = 0.68869;

l17 = 0.70002;

l18 = 0.68869;
l19 = 0.65387;
l20 = 0.59280;
l21 = 0.49931;
l22 = 0.35661;

%opgelegde load
q_oload = F/(4*b_last);
N_oload = q_oload*a;
sigma_oload = N_oload/A;
display(q_oload);
display(N_oload);
display(sigma_oload/(1e6));
m_oload = F/g;
display(m_oload);

%buckling check
N_bmax = ((pi^2)*E*I)/(L_b^2); %normaalkracht in N
display(N_bmax);
q_bmax = N_bmax/a;
display(q_bmax);
m_bmax = (q_bmax*4*b_last)/g;
display(m_bmax);
```